Journal of Engineering and Applied Science

RESEARCH Open Access

Fatigue behavior of surfaced C45 steel

A. A. Sayid[1], E. El-Kashif[1], M. A. Adly[1], M. A. Morsy[2] and Abdallah Abdelkawy[1*]

* Correspondence: abdallah.abdelkawy@ejust.edu.eg
[1]Mechanical Design and Production engineering, Faculty of Engineering, Cairo University, Giza, Egypt
Full list of author information is available at the end of the article

Abstract

Due to the dynamic loads in power transmission such as automotive, the restoration of axles during maintenance is extensively needed. These parts face two main challenges: wear and fatigue failure loads. The present study tries to improve fatigue strength of C45 steel by surfacing with tungsten inert gas (TIG) welding technique using filler ER80S-B2. Fatigue life was studied through a rotary bending fatigue test at two stress levels: level I 65% and level II 55% of the ultimate tensile strength of C45 base steel. Loading amplitude, coating thickness, surface roughness, and rotating speed were kept constant for all specimens. In accordance with ISO 12107, both surfaced and unsurfaced steel fatigue specimens were prepared. The specimens were tested till failure and the data were analyzed. The chemical composition, tensile strength, micro-hardness, microstructure, and fracture surface have been examined for surfaced and unsurfaced steels. Surfaced C45 steel showed improved fatigue life compared to the unsurfaced C45 steel specimens with an increasing percentage of 35.97% at level I and 25.46% at level II.

Keyword: C45 steel, Surfacing, Reclamation, Microstructure, Fatigue life

Introduction

Nowadays, increasing the needs for the applications exposed to dynamic loads such as rotating, vibrated, and impacted parts which are subjected to high fatigue loads directed the researchers to study fatigue stresses and methods to overcome these stresses [1–4]. The machinery subjected to the fatigue stresses are also suffering from generated temperatures as transportations, manufacturing machines, and power generation stations which increases the dramatic effect of the fatigue stresses [5, 6]. Fatigue life and the related aspects as the wear resistance were investigated experimentally and mathematically.

In this regard, Ligaj et al. studied the fatigue life for C45 steel and formulated it based on the high-cyclic load by the stresses, low-cyclic load using strain, and a mixture of stress and strain. Then, they investigated experimentally the fatigue life at maximum stress 650 MPa, 570 MPa, 460 MPa, and 340 MPa [7]. Al-Fadhli et al. investigated the effect of Inconel-625 alloy coating for stainless steel on fatigue and corrosion. They found that the immersion of the coated samples in corrosive solution reduces the fatigue life [8]. Robak et al. introduce a model to predict the fatigue life of

ring-notched elements within a range from 10^4 to 10^6. They verified their model by carrying experiments on C45 [9]. Marcisz et al. investigated the fatigue life of C45 steel under cyclic through controlled energy parameters. They derived a model that correlates the number of cycles up to failure and the applied energy [10].

Researchers invented some methods to improve the fatigue life of different materials. In this regard, Kumar et al. used the TIG welding method to surface samples from AISI 4340 alloy steel. They found that this surfacing method improved the fatigue life by about 40% compared to the base alloy [11]. Puchi-Cabrera investigated the effect of coating SAE 4340 steel alloy with TiCN by ion plating. The fatigue strength of the coated samples was greater compared to the uncoated samples due to the increase in the yield strength. The crack is started at the film of TiCN firstly which has higher strength then reaching to the substrate [12].

There are many techniques used to improve the fatigue strength of C45 steel; Bartkowski et al. produced coated C45 steel by silicon and boron powder with different percentages using the laser. They found that coating with silicon only produced lower micro-hardness compared to the boron coating as there is no hard phase in the case of the Fe-Si equilibrium phase diagram. Hence, the wear rate in the case of silicon was higher compared to the other coating percentages [13]. Moreover, Chapetti et al. studied the effect of ultra-fine grain size on the fatigue life using ultra-fine-grained low steels. They found that the reduced grain size increased the fatigue strength since the smooth fatigue limit is dependent on the ability of the first grain boundary to stop the micro-cracks propagation [14]. Other researchers tried to just change the experimental conditions not treating the samples. Ranc et al. investigated the fatigue life at different ultrasonic vibration amplitudes with and without compressed air as a cooling. They concluded that the fatigue life increased to 10^{10} cycles compared to 2×10^8 which was found in the review, and there is no significant difference between cooled and not cooled samples. Moreover, they found that the self-heating temperature increased with the stress amplitude [15]. Tomkom et al. studied the wear, hardness, and microstructure for S355G10+N steel coated with Omnia and barracuda gold, and the welding process was performed underwater and in air. They found that the coating in air produces a ferritic-pearlitic structure with fine grains due to the low cooling rate. This structure is characterized by high wear resistance compared to the pearlite structure which formed in the case of underwater welding [16]. Zaleski et al. studied the effect of shot peening on the wear resistance and fatigue life for C45 steel. They found that this technique increased the fatigue life greatly compared to the ground specimens [17]. Sano et al. compared the fatigue strength for A6061-T6 aluminum alloy and the application of laser peening without a coating which results in prolonged fatigue life by about 50% compared to the base metal [18].

In this paper, surfacing C45 steel alloy which is dedicated for the automobile axels through welding method is introduced to improve the fatigue strength. The effect of the surfacing parameters is investigated by testing tensile test, micro-hardness, microstructure, and fatigue strength testing at two stress levels.

Methods

This section describes the used materials and experimental and testing methods. The base material used in this study was C45, which is a medium carbon steel with high

strength and hardness. The chemical composition of the steel used is given in Table 1. The surfacing material used was ER80S-B2 (Select Arc Welding Industries, FSH Welding Group, France) based on AWS A5.28, and its material number is 1.7338 according to DIN. The typical chemical composition for the surfacing material is shown in Table 1. The weld metal mechanical properties according to its datasheet and the used welding parameters are shown in Table 2.

The C45 specimens were preheated to 230 °C before surfacing which was calculated using Seferian's formula shown in Eq. (1) [19]:

$$T_{\text{preheating}}\,(^{\circ}\text{C}) = 350\sqrt{(C_e - 0.25)} \tag{1}$$

where C_e is the modified carbon equivalent, and it is equal to the summation of the chemical carbon equivalent C_k and test piece thickness effect (C_d). The chemical carbon equivalent C_k can be calculated from Eq. (2):

$$C_k = C + \frac{Mn + Cr}{9} + \frac{Ni}{18} + \frac{7{*}Mo}{90} \tag{2}$$

The base metal specimens were prepared according to the instruction of rotating-beam bending fatigue testing machine model RBF-200 HT (System Integrator LLC, USA) as shown in Fig. 1. Another set of samples was prepared for surfacing by reducing the gauge zone diameter to 5 mm followed by surfacing and finally turned to 6.35 mm diameter to be compared with the base samples under the same testing conditions.

Tensile test was performed according to ISO 6892-1 standards for both base and welded metals using a 10-kN (Shimadzu, AG-X/R Autograph, Japan) universal testing machine. The cross-head speed was 5 mm/min. The tensile test was carried out for three samples of each condition, and the average was taken. The micro-hardness test was carried out using Vickers hardness measurements with polished samples from the base and surfaced materials following ASTM E384-11. The load was 100 g/f and a dwell time of 10 s to observe the hardness distribution through the weld metal, HAZ, and the core of sample; the reported hardness values were the average of at least five measurements.

All the specimens were tested using a rotating bending fatigue machine model RBF-200 HT at the stress levels shown in Table 3 with stress ration, $R = -1$. For steels, the expected endurance limit is equal to half the ultimate tensile strength (UTS) provided that UTS is lower than 1460 MPa [20]. The two stress levels were selected above the expected endurance limit to achieve high stress level fatigue, and the results were recorded as the number of cycles to failure corresponding to the stress level used.

Different microstructures of surfaced and unsurfaced material were examined using an optical microscope. The samples were cut and mounted in bakalite. After that, samples were ground and polished manually then etched in 2% Nital. Energy-dispersive X-ray spectroscopy EDS attached with Bruker AXS-Flash Detector 410-M, Germany, was utilized for base metals and surfaced metal. The fatigue fracture surfaces of failed test

Table 1 Typical chemical composition, wt%

Chemical elements %	C	Si	Mn	P	S	Cr	Mo	Ni	Cu	Fe
Base metal (C45)	0.438	0.286	0.743	0.01	0.03	0.2	0.006	0.023	0.005	Bal.
Surfacing material (ER80S-B2)	0.09	0.6	0.6	0.01	0.01	1.3	0.5	0.03	0.2	Bal.

Table 2 Mechanical properties and welding parameters

Mechanical properties			Welding parameters				
Tensile strength (MPa)	Yield strength (MPa)	Elongation %	Process	Wire diameter (mm)	Ampere (A)	Voltage (V)	Gas
590	490 MPa	25%	TIG	1.6 mm	50–120	7~13	Ar

specimens: unsurfaced and surfaced were studied by scanning electron microscope (SEM) model FEI Inspect S50, Netherlands.

Results and discussion

This section shows the results and the discussion related to the pre-described experiments. Steel C45 after surfacing are analyzed, and its composition is shown in Table 4. The analysis shows compatible results with the standard EN 10083-2: 2006 of the chemical composition of C45 steel shown before in Table 1.

By using the carbon equivalent equation mentioned before, the carbon equivalent is 0.57% and the chemical composition of the surfaced layer shows almost no dilution, and this is the target of choosing this wire to get minimum dilution so that both surfaced and HAZ regions have similar chemical composition, microstructure, and mechanical properties.

Microstructural characterization and micro-hardness distribution

The main factors affecting the microstructure of the weld are the chemical composition of the base metal and the filler besides the cooling rate. In order to enhance the mechanical properties of surfaced medium carbon steel, the selection of suitable wire composition plays a very important role in obtaining fine acicular ferrite (lower bainite); this bainitic structure has been proven to improve the performance of such surfacing especially under fatigue loading [21]. The microstructure of C45 steel base metal is a ferritic pearlitic structure as shown in Fig. 2a which is the result of annealing in the as-received condition. The amount of ferrite is about 44%, and the amount of pearlite is about 56% according to phase rule calculations.

Figure 2b–d show three microstructure zones, Fig. 2b shows the core of the specimen which is perlite (black) with thin pro-eutectoid grain boundary ferrite (white) while Fig. 2c shows the interface zone microstructure which is a pearlite, thin grain boundary ferrite, and Widmanstatten ferrite. Figure 2d shows the microstructure of the surfaced layer which is Widmanstatten ferrite. The different microstructures obtained are mainly due to the different chemical compositions and heat cycles.

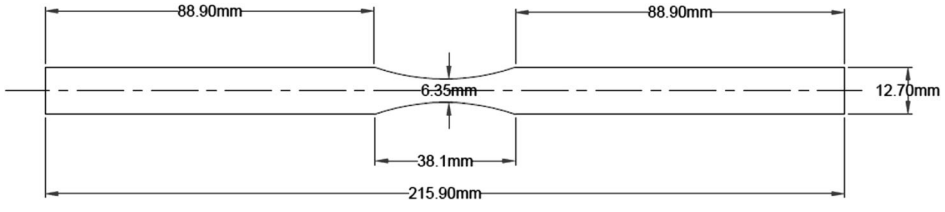

Fig. 1 Fatigue sample dimensions in mm

Table 3 Stress levels of fatigue test specimens

Steel	No. of specimens of fatigue tests		Stress (MPa)	Percentage of UTS
C45	20 for unsurfaced	10 for level I stress	489.45	65%
		10 for level II stress	414.15	55%
	20 for surfaced	10 for level I stress	489.45	65%
		10 for level II stress	414.15	55%

When the coarse-grained austenitic steel is rapidly cooled due to high-temperature heating but below the critical cooling rate, the typical microstructure formed is called Widmanstatten structure. In this configuration, the proeutectoid phase is separated not only along the grain boundary of the austenite, but also in the shape of the plate or the needle in a certain crystal face and direction to form a mesh arrangement. The higher mechanical properties of steels with a Widmanstatten structure are attributed to the fine grain structure of the ferrite and the higher percentage of quasi-eutectoid [7].

Tensile test and micro-hardness

Figure 3 shows the micro-hardness distribution of C45 surfaced steel specimens at the test section which includes the surfaced layer, interface zone, and the core. It is clear from the micro-hardness results that the surface layer is harder than the core.

Circular cross-sections were taken just behind the facture surface for micro-hardness testing, and the readings were taken at 0.1 mm step from the interface between base and surface area in both directions as shown in Fig. 3; the black line represents the hardness of the surface area while the red line represents both the base metal and the heat-affected zone. No interpolation was used, and each reading is the average of 5 readings. The high hardness is related to a higher fatigue strength of C45 surfaced specimens as explained according to Eq. (3):

$$\sigma_w = 1.6\mathrm{HV} + 0.1\mathrm{HV} \tag{3}$$

where σ_w is the fatigue limit (MPa) and HV is the Vickers hardness in MPa.

The relationship of Eq. (3) between hardness and fatigue limit is assessed to be reliable for HV < 400. However, for HV > 400, no definite correlation with HV could be found [8].

The ultimate tensile strength (UTS) increases from 753 MPa for the base metal to784 MPa in case of C45 surfaced which supports the expectation of improving the number of cycles to failure and strength in the surfaced specimens more than base metal specimens.

Fatigue testing

Table 5 shows the results of 10 specimens C45 (BM) fatigue life at level I stress 65% and at level II stress 55%. The mean value of the number of cycles to failure for the samples is calculated, and the improvement due to the surfacing treatment is found. This treatment improves the number of cycles to failure by about 36% at the lower

Table 4 Chemical composition of C45 steel after surfacing (wt%)

C	Si	Mn	P	S	Cr	Ni	Fe
0.438	0.286	0.743	0.0106	0.0285	0.194	0.0226	Bal.

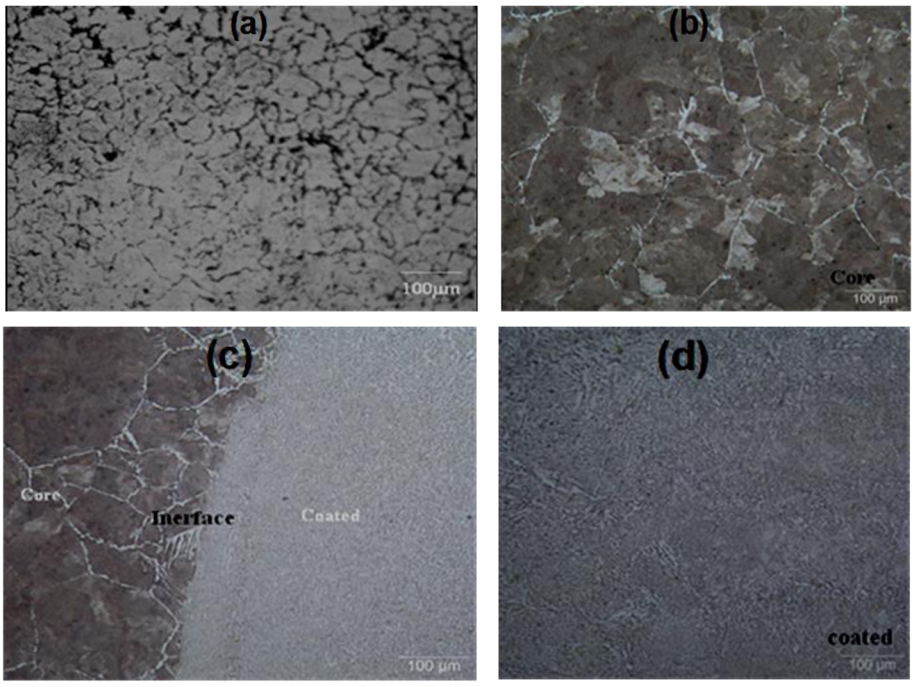

Fig. 2 **a** As-received C45 steel ferritic pearlitic microstructure. **b** Core microstructure, pearlite (black), and thin grain boundary ferrite (white). **c** Interface microstructure, Widmanstatten ferrite (surfaced) and pearlite, and thin grain boundary ferrite (core). **d** Surfaced microstructure Widmanstätten ferrite

stress level and by about 25% at the higher stress level. Figure 4 supports the findings listed in Table 5.

Figure 5 shows the fatigue strength versus the number of cycles to failure curve at two stress levels for C45 base steel and surfaced; it shows that the surfaced C45 is shifted to the right compared with the C45 steel. Comparing the number of cycles to failure between C45 steel base metal (BM) and C45 steel surfaced by using TIG welding showed that for similar stress, C45 surfaced specimens exhibited a higher number of cycles to failure compared to the specimens of C45 (BM). This phenomenon is

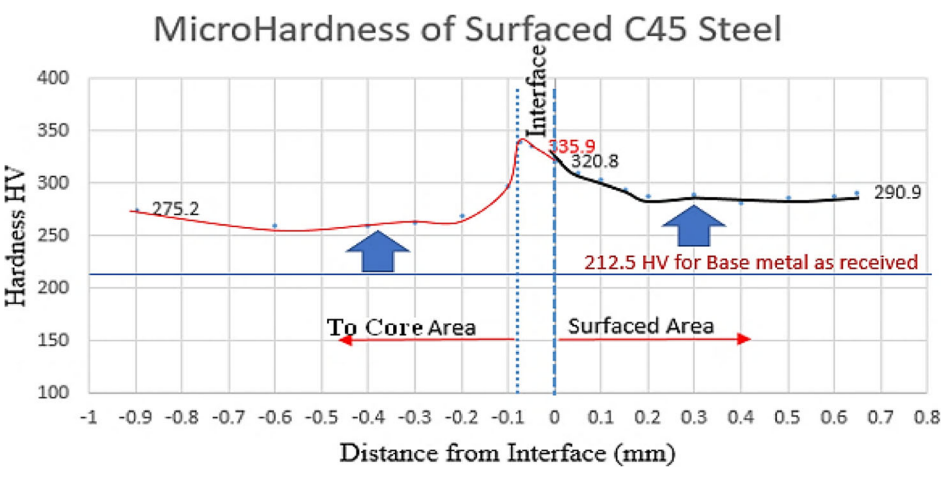

Fig. 3 Micro-hardness of C45 surfaced (S)

Table 5 Fatigue test results of C45 steel (BM and surfaced)

Stress level	Stress (MPa)	No.	Number of cycles to failure for base metal C45 (*N*) (10^4)		Number of cycles to failure for surfaced C45 steel (*N*) (10^4)		Number of cycles impartment
			For samples	Mean	For samples	Mean	
65% of UTS of C45 base metal	489.45	1	2.03	4.85	10.1	6.59	35.97%
		2	3.43		5.60		
		3	2.81		7.37		
		4	5.37		10.1		
		5	1.07		8.24		
		6	2.34		3.51		
		7	6.30		6.59		
		8	4.32		4.29		
		9	8.04		2.43		
		10	31.2		7.71		
55% of UTS of C45 base metal	414.15	1	13.3	14.7	8.43	18.5	25.46%
		2	13.4		28.6		
		3	11.3		27.9		
		4	19.6		17.6		
		5	12.2		30.0		
		6	18.4		15.9		
		7	14.4		8.38		
		8	16.4		18.9		
		9	15.9		5.67		
		10	12.3		23.3		

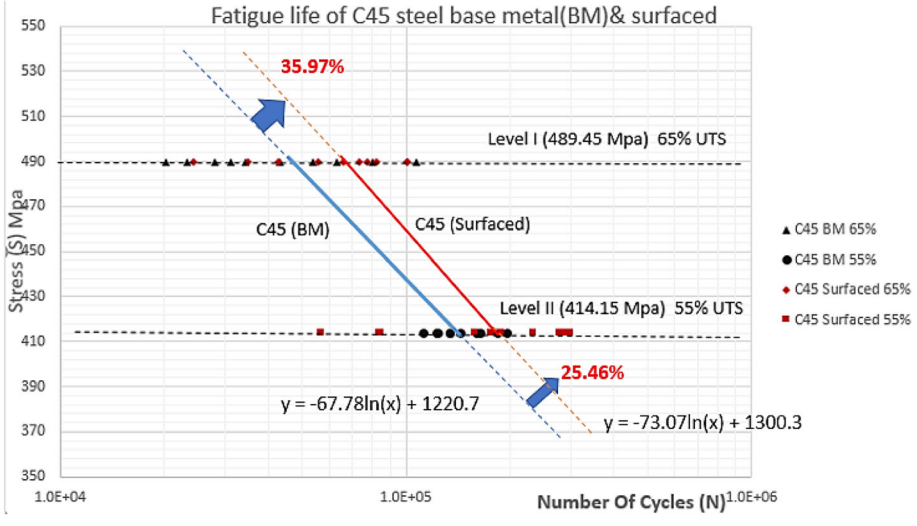

Fig. 4 Rotating bending fatigue results for C45 steel (BM and surfaced) at two levels of stress and the confidence levels for each condition

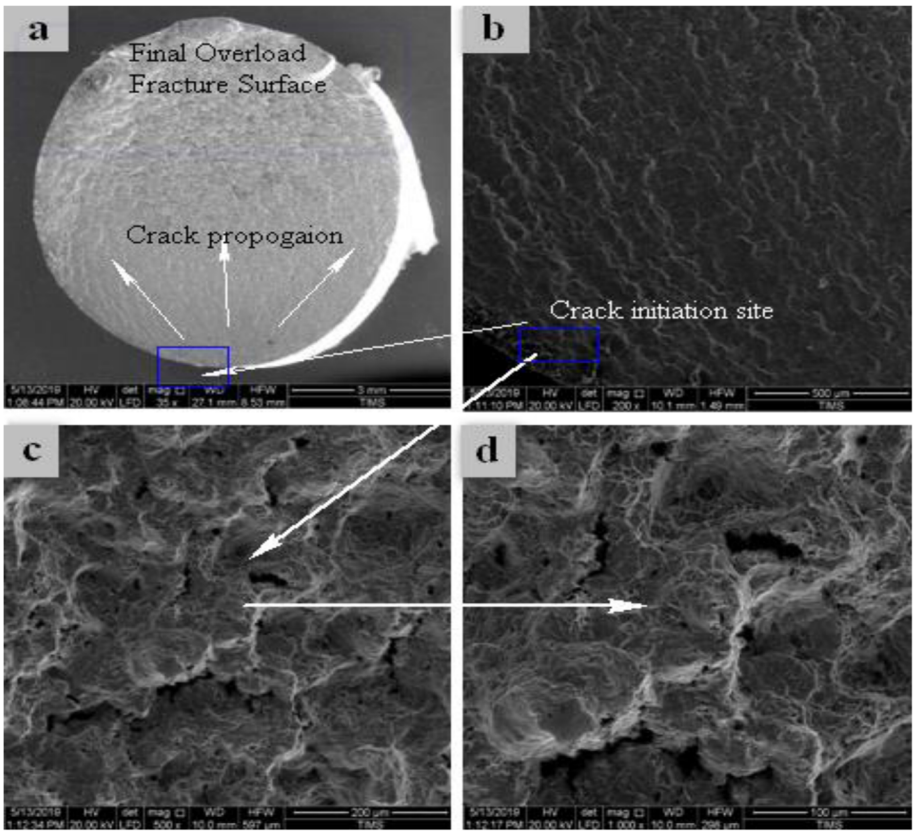

Fig. 5 **a** Fracture surfaces of C45 (BM) fatigue specimen at $N = 133{,}500$. **b** Crack initiation site. **c** Cleavage fracture. **d** Magnification of the initiation site

expected to occur due to the formation of Widmanstätten ferrite at surfaced layer, and the Widmanstatten structure has higher strength, higher hardness, and better plasticity characteristics than steel with a ferrite-pearlite structure which form the C45 base metal.

The confidence interval for the results shown in Fig. 4 is listed in Table 6.

Fatigue samples, base metal and surfaced, tested at 55% and 65% stress levels were analyzed by SEM techniques to investigate more closely the microstructure characteristics of the crack initiation sites, and the general microstructure changes happened during the propagation of these cracks on subsequent sample cross-sections. Figure 5 shows SEM micrographs for fatigue failure of C45 base metal specimens. Figure 5a, b show the formation of a crack near the outer surface; however, the smooth region near the crack initiation site and the arrows indicate the crack propagation direction to the final fracture area. The fracture surface is examined and shown cleavage fracture which

Table 6 Confidence intervals for each stress level used for both base metal and surfaced samples

Material conditions	Stress levels (MPa)	Upper confidence level	Lower confidence level
Base metal	489.45	130,357	3463
	414.15	167,055	127,344
Surfaced samples	489.45	84,759	47,120
	414.15	248,743	120,616

is the characteristic of brittle fracture as a result of bending fatigue test as shown in Fig. 5c, d.

The fracture surface of the surfaced specimens shows a change in the crack propagation path compared to the unsurfaced or base specimen as shown in Fig. 6. The initial crack is formed near the surface as shown in Fig. 6a, b. The coarse region near the crack initiation site and the arrows indicate the crack propagation to the final fracture area. The fracture surface is examined, and it shows the cleavage fracture which is the characteristic of brittle fracture and dimple fracture which is the characteristic of ductile fracture as a result of bending fatigue test as shown in Fig. 6b, c. This mixed mode of fracture is the cause of long number of cycles to failure obtained for the surfaced C45 steel compared with the unsurfaced one.

The fracture surface of the surfaced specimens shows a change in the crack propagation path compared to the base steel specimen. The presence of the final rupture zone of circular or elliptical geometry in all fractured surfaced samples provides a strong indication that the crack propagates in a circular progression in the sample before

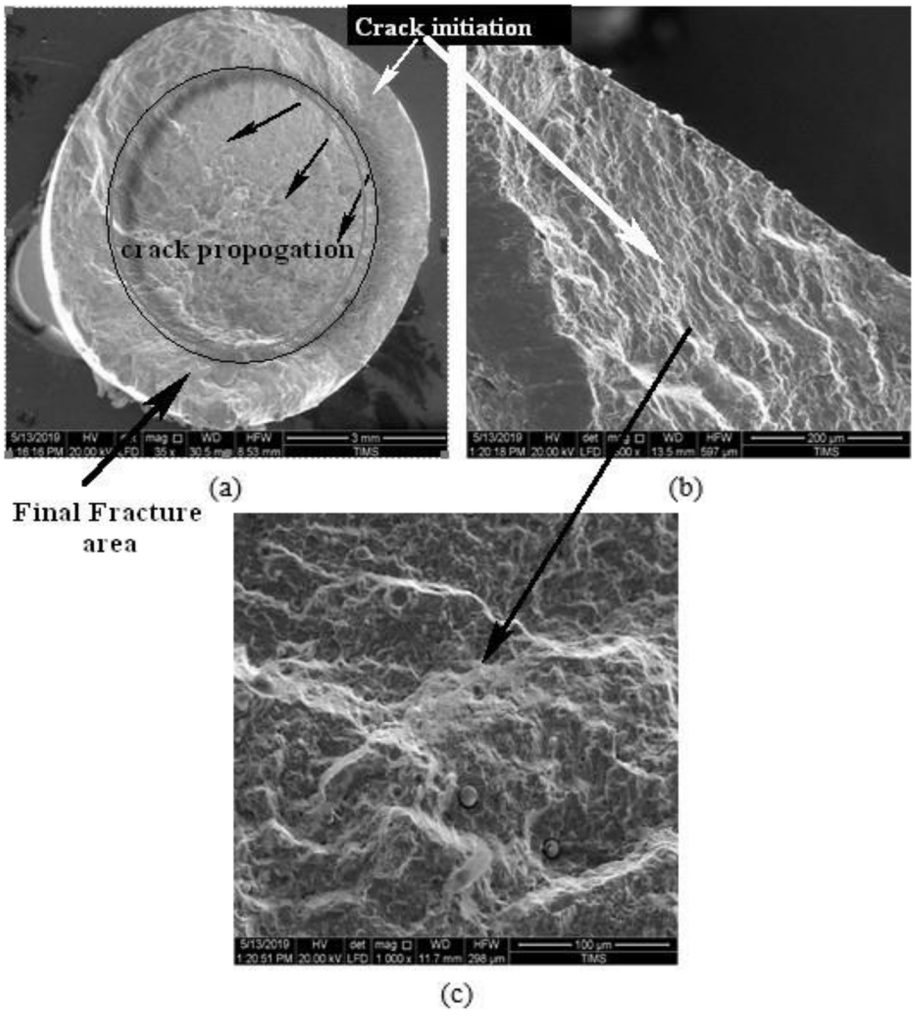

Fig. 6 **a** Fracture surfaces of C45 (S) fatigue specimen at $N = 279{,}200$. **b** Crack initiation site. **c** Mixed fracture modes: cleavage and dimple fracture

complete fracture. This circular motion occurs due to the weld deposit of the coating on the surface of the sample. The interface between the coating and the substrate acts as a circumferential stress concentration location that distributes the stress evenly around the outer diameter of the substrate. Therefore, surfacing could affect the mechanical properties of the C45 steels superiorly based on the resulting microstructure at both core and surface after surfacing and also on the hardness distribution, which determines the fatigue behavior of the steel studied.

Conclusions

Fatigue behavior of surfaced C45 with ER80S-B2 filler by TIG welding process was investigated at two stress levels of 55% and 65% from their base steels' ultimate tensile strength, and the following can be concluded:

1. Surfaced C45 steel exhibits better fatigue failure resistance and longer number of cycles to failure than base steel due to the formation of Widmanstätten ferrite at the surface while the core remains pearlitic-ferritic structure.
2. Tensile strength and micro-hardness of surfaced C45 are improved significantly compared to C45 base steel.

Abbreviations

$T_{preheating}$: Preheating temperature for before surfacing; C_e: Modified carbon equivalent; C_k: Chemical carbon equivalent; C_d: Test piece thickness effect; HAZ: Heat-affected zone; HV: Vickers's Hardness; σ_w: Fatigue limit; BM: Base metal; ASTM: American Society for Testing and Materials; UTS: Ultimate tensile strength; TIG: Tungsten inert gas; S-N curve: Stress versus the number of cycles to failure; SEM: Scanning electron microscope

Acknowledgements

The authors are very grateful to Prof. Chahinaz Abd El-Rahman, Faculty of Engineering-Cairo University, for her advices, support, and fruitful discussion during this work.

Authors' contributions

AAS has performed the microstructure, hardness, tensile, and fatigue testing for this manuscript. MA suggested the paper idea and the methodology of the research. MM helped in the observation of the SEM fracture surface. EE explained the microstructure in the as-received condition and the metallurgical changes after welding. AA wrote the paper, analyzed and discussed the results, and explained the mechanical behavior based on the microstructure obtained after welding. All authors have read and approved the final manuscript.

Funding

This study had no funding from any resource.

Availability of data and materials

All data are available.

Declaration

Competing interests

The authors declare that they have no competing interests.

Author details

[1]Mechanical Design and Production engineering, Faculty of Engineering, Cairo University, Giza, Egypt. [2]Central Metallurgical Research and Development Institute, El-Tebein, Cairo, Egypt.

Received: 25 March 2021 Accepted: 8 August 2021
Published online: 21 October 2021

References

1. Rajanna K, Kolsters B (1991) Fatigue fracture surface analysis C45 steel specimens using X-ray. Eng Fracture Mech 39(I): 147–157. https://doi.org/10.1016/0013-7944(91)90030-5
2. Föhl J, Weissenberg T, Wiedemeyer J (1989) General aspects for tribological applications of hard particle coatings. Wear 130(2):275–288. https://doi.org/10.1016/0043-1648(89)90183-X
3. Contreras G, Fajardo C, Berrios J, Pertuz A, Chitty J, Hintermann H, Puchi E (1999) Fatigue properties of an AISI 1045 steel coated with an electroless Ni-P deposit. Thin Solid Films 355:480–486. https://doi.org/10.1016/S0040-6090(99)00672-0

4. Seleem M, Ahmed S, Sallam H, Moshref S, Haroun M (2007) Fatigue crack growth behavior under variable amplitude loading. J Eng Appl Sci Fac Eng Cairo Univ 54:579–598
5. Gallo P, Berto F (2015) Advanced materials for applications at high temperature: fatigue assessment by means of local strain energy density. Adv Eng Mater 12:1557–1564
6. Meneghetti G, Ricotta M, Atzori B (2016) A two-parameter, heat energy-based approach to analyse the mean stress influence on axial fatigue behaviour of plain steel specimens. Int J Fatigue 82:60–70. https://doi.org/10.1016/j.ijfatigue.2015.07.028
7. Ligaj B, Szala G (2012) Comparative analysis of fatigue life calculation methods of C45 steel in conditions of variable amplitude loads in the low- and high-cycle fatigue ranges. Polish Maritime Res 19(4):23–30
8. Al-fadhli H, Stokes J, Hashmi M, Yilbas B (2006) HVOF coating of welded surfaces: fatigue and corrosion behaviour of stainless steel coated with Inconel-625 alloy. Surf Coat Technol 200(16-17):4904–4908. https://doi.org/10.1016/j.surfcoat.2005.04.052
9. Robak G (2020) Using a variable value of the fictitious radius to estimate fatigue life of notched elements. Fatigue Fract Eng Mater Struct 43(9):2006–2023. https://doi.org/10.1111/ffe.13280
10. Marcisz E, Marciniak Z, Rozumek D, Macha E (2014) Energy fatigue characteristic of C45 steel subjected to cyclic bending. Key Eng Mater 598:147–152. https://doi.org/10.4028/www.scientific.net/KEM.598.147
11. Kumar S, Ghosh P (2018) TIG arc processing improves tensile and fatigue properties of surface modified of AISI 4340 steel. Int J Fatigue 116:306–316
12. Puchi-Cabrera E, Staia M, Quinto D, Villalobos-Gutiérrez C, Ochoa-Pérez E (2007) Fatigue properties of a SAE 4340 steel coated with TiCN by PAPVD. Int J Fatigue 29(3):471–480. https://doi.org/10.1016/j.ijfatigue.2006.05.003
13. Bartkowski D, Bartkowska A, Popławski M, Przestacki D (2020) Microstructure, microhardness, corrosion and wear resistance of B, Si and B-Si coatings produced on C45 steel using laser processing. Metals (Basel) 10:1–17
14. Chapetti M, Miyata H, Tagawa T, Miyata T, Fujioka M (2004) Fatigue strength of ultra-fine grained steels. Mater Sci Eng A 381(1–2):331–336. https://doi.org/10.1016/j.msea.2004.04.055
15. Ranc N, Favier V, Munier B, Vales F, Lefebvre F (2015) Thermal response of C45 steel in high and very high cycle fatigue. Proc Eng 133:265–271. https://doi.org/10.1016/j.proeng.2015.12.668
16. Tomków J, Czupryński A, Fydrych D (2020) The abrasive wear resistance of coatings manufactured on high-strength low-alloy (HSLA) offshore steel in wet welding conditions. Coatings 10:1–13
17. Zaleski K (2017) The effect of vibratory and rotational shot peening and wear on fatigue life of steel. Maintainance Reliability 19(1):102–107. https://doi.org/10.17531/ein.2017.1.14
18. Sano Y, Masaki K, Gushi T, Sano T (2012) Improvement in fatigue performance of friction stir welded A6061-T6 aluminum alloy by laser peening without coating. Mater Des 36:809–814. https://doi.org/10.1016/j.matdes.2011.10.053
19. Skumavc A, Tušek J, Nagode A, Kosec L (2013) Tungsten heavy alloy as a filler metal for repair welding of dies for high pressure die casting. Int J Mater Res 104(11):1143–1150. https://doi.org/10.3139/146.110963
20. Budynas RG, Nisbett JK (2015) Shigley's mechanical engineering design. Mc Graw Hill.
21. Casagrande A, Cammarota G, Micele L (2011) Relationship between fatigue limit and Vickers hardness in steels. Mater Sci Eng A 528(9):3468–3473. https://doi.org/10.1016/j.msea.2011.01.040

Publisher's Note